

## The Optical Gravitational Lensing Experiment. Optical Counterparts to the X-ray Sources in the Galactic Bulge \*

A. Udalski<sup>1</sup>, K. Kowalczyk<sup>1</sup>, I. Soszyński<sup>1</sup>, R. Poleski<sup>1</sup>,  
M. K. Szymański<sup>1</sup>, M. Kubiak<sup>1</sup>, G. Pietrzyński<sup>1,2</sup>,  
S. Kozłowski<sup>1</sup>, P. Pietrukowicz<sup>1</sup>, K. Ulaczyk<sup>1</sup>,  
J. Skowron<sup>3,1</sup>, and Ł. Wyrzykowski<sup>1</sup>

<sup>1</sup>Warsaw University Observatory, Al. Ujazdowskie 4, 00-478 Warszawa, Poland  
e-mail: (udalski, kowalczyk, soszynsk, rpoleski, msz, mk, pietrzn, simkoz, pietruk,  
kulaczyk, jskowron, wyrzykow)@astrouw.edu.pl

<sup>2</sup>Universidad de Concepción, Departamento de Astronomía, Casilla 160-C, Concepción,  
Chile

<sup>3</sup>Department of Astronomy, Ohio State University, 140 W. 18th Ave., Columbus,  
OH 43210, USA

### ABSTRACT

We present a sample of 209 variable objects – very likely optical counterparts to the X-ray sources detected in the direction of the Galactic center by the Galactic Bulge Survey (GBS) carried out with the Chandra satellite. The variable sources were found in the databases of the OGLE long term survey monitoring regularly the Galactic bulge since 1992. The counterpart candidates were searched based on the X-ray source position in the radius of  $3''9$ .

Optical light curves of the candidates comprise a full variety of variability types: spotted stars, pulsating red giants (potentially secondary stars of symbiotic variables), cataclysmic variables, eclipsing binary systems, irregular non-periodic objects including an AGN (GRS 1734–292).

Additionally, we find that positions of 19 non-variable stars brighter than 16.5 mag in the OGLE databases are so well aligned with the X-ray positions ( $< 0''.75$ ) that these objects are also likely optical counterparts to the GBS X-ray sources.

We provide the OGLE astrometric and photometric information for all selected objects and their preliminary classifications. Photometry of the candidates is available from the OGLE Internet archive.

**Key words:** *X-ray: stars – X-ray: binaries – Stars: activity – binaries: symbiotic – novae, cataclysmic variables – Galaxies: Seyfert*

---

\*Based on observations obtained with the 1.3 m Warsaw telescope at the Las Campanas Observatory of the Carnegie Institution for Science.

## 1. Introduction

Recent years have been witnessing an enormous progress in the X-ray astronomy thanks to many satellite missions with continuously more sensitive state-of-the-art detectors. The number of detected X-ray sources increased rapidly. For example, the surveys of the Magellanic Clouds led to the discovery of tens of new X-ray pulsars (Coe *et al.* 2005) and AGNs (Kozłowski *et al.* 2012), Galactic center survey discovered more than thousand new X-ray sources toward the Galactic center (Jonker *et al.* 2011), the XMM-Newton catalog of serendipitous X-ray sources includes almost 200 000 objects (Watson *et al.* 2009),

Proper classification and then interpretation of an X-ray source usually requires additional observations in other wavelength bands, usually in the optical or IR range. Therefore, it is crucial to find the X-ray source counterparts in these bands, if the data exist.

The accuracy of positions of X-ray sources detected by the modern instruments is comparable to that obtained in the optical range. This in principle can make the cross-identification of the optical counterparts relatively straightforward. Indeed, it is often true in empty stellar fields, where the X-ray position unambiguously points to an object. The situation is, however, much more difficult in dense stellar fields such as the Magellanic Clouds or Galactic center, where one can detect even several dozen objects within the X-ray position error box. In such cases positive cross-identification can often be non-trivial.

On the other hand, the photometric variability of an object located close to the X-ray source position can be a very good indicator of its close relation with the detected X-ray source. It is well known that many different types of variable objects emit X-rays, for example, all types of cataclysmic variables, low and high mass X-ray binaries, chromospherically active and spotted stars, long period variables etc. Thus, the detection of optical variability in an object located in the X-ray position error box practically proves correctness of the cross-identification.

What is more important, variability provides many additional information on the X-ray system for its proper classification and detailed studies of its structure. For example, the detected periodicities can be interpreted as related to orbital or rotational periods. Observed flares or flickering can provide information on the rapid phenomena occurring in accreting systems or on stellar chromospherical activity.

Here, we present the results of our search for variable objects located at the positions of the X-ray sources detected by the Galactic Bulge Survey (GBS, Jonker *et al.* 2011). Altogether, we have found 209 variable optical objects that can be considered as the optical counterparts to X-ray sources detected by the GBS survey. For all of them we provide their basic classification and light curve parameters. The photometric data are available from the OGLE Internet archive (see Section 5).

## 2. Observational Data

The X-ray sources analyzed in this paper were detected by the GBS project (Jonker *et al.* 2011). They list 1234 sources detected by the Chandra satellite in two regions located symmetrically along the Galactic plane:  $-3^\circ < l < 3^\circ$ ,  $1^\circ < |b| < 2^\circ$ , *i.e.*, covering 12 square degrees near the Galactic center and avoiding the highest extinction regions close to the Galactic plane. The GBS catalog provides the positions of the detected sources with typical accuracy of about  $0''.25$  in right ascension and declination, although in rare single cases the accuracy of position can be worse than  $1''.5$ .

The main optical dataset comes from the fourth phase of the Optical Gravitational Lensing Experiment (OGLE-IV). Observations were collected between March 2010 and June 2012 (and the data are still being collected as the OGLE-IV project continues). The 1.3-m Warsaw Telescope located at Las Campanas Observatory, Chile, operated by the Carnegie Institution for Science was used with the OGLE-IV 32-chip mosaic camera covering approximately 1.4 square degrees on the sky with the scale of 0.26 arcsec/pixel.

As the OGLE-IV survey focuses on variability, observations have been carried out mostly in the *I*-band filter. About 10% images are taken in the *V*-band to secure color information. The cadence of observations depends on the field. In the regions where the gravitational microlensing phenomena (main target of the OGLE-IV survey in the Galactic bulge) occur most frequently the cadence is very high reaching one observation per 18 minutes. Other fields are observed less frequently but typically not less than one observation per one/two nights during the mid observing season is obtained. The OGLE-IV light curves presented here have from more than 5000 to 100 epochs in the highest and lowest cadence fields, respectively.

Fig. 1 shows the map of the Galactic center with the coverage by the OGLE-IV survey. It can be compared with the map of GBS survey coverage (Fig. 1, Jonker *et al.* 2011).

The exposure time of *I*-band images was set to 100 s and to 150 s for the *V*-band frames. Because of very high stellar density, observations of the Galactic bulge are conducted only during good seeing (less than  $1''.8$ ) and transparency conditions.

Photometry of all objects located in the OGLE-IV Galactic center fields is derived with the image subtraction method (Alard and Lupton 1998, Alard 2000, Wozniak 2000). The data pipeline is based on slightly modified OGLE-III data pipeline (Udalski 2003). At the time of this analysis photometry of the fields marked with the red borders in Fig. 1 was accessible. The databases of these 58 OGLE-IV fields contain photometry of about 250 million stars. OGLE-IV photometry has so far been only roughly calibrated and the uncertainty of the zero point may reach 0.1–0.15 mag.

Astrometry of the OGLE-IV fields was derived in the identical way as for the OGLE-III photometric maps (Szymański *et al.* 2011) and tied to the 2MASS survey coordinate system. Comparison of the positions obtained for thousands of cross-

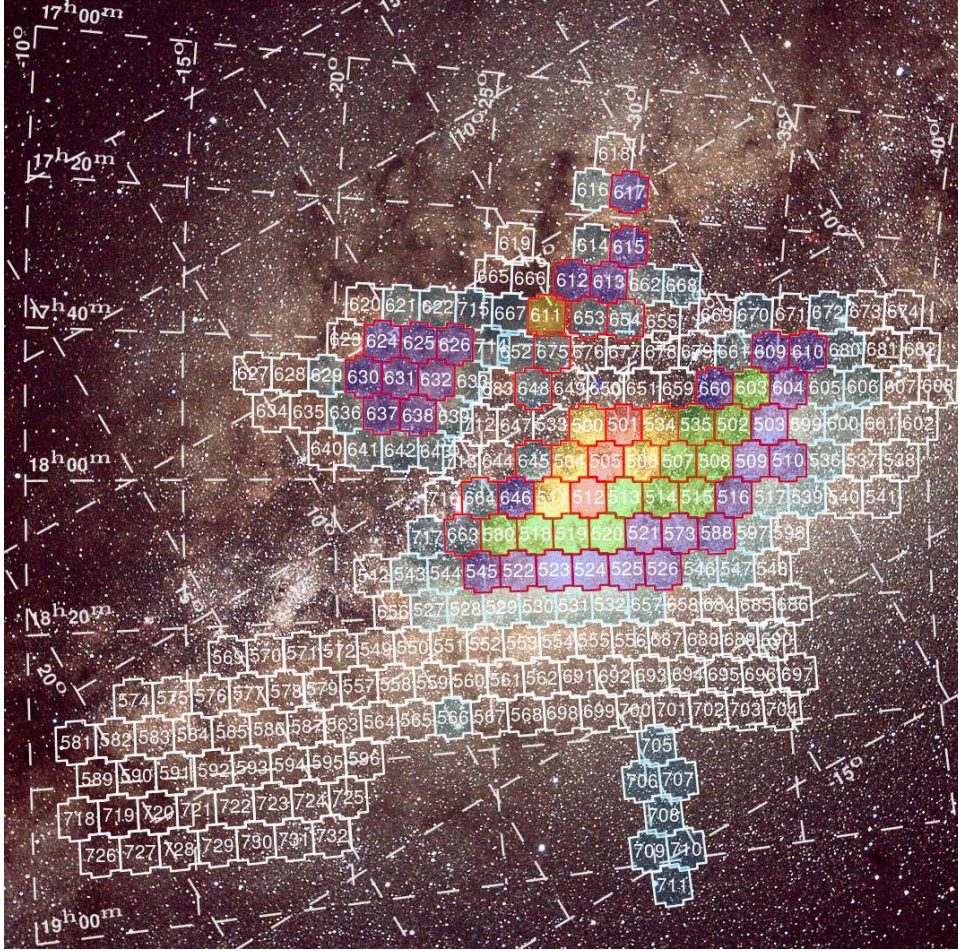


Fig. 1. Map of the fields observed by the OGLE-IV survey in the Galactic bulge colored according to the cadence of observations. Dashed white lines mark the equatorial and Galactic coordinate grids (every  $5^\circ$  in  $l$  and  $b$ ). Red field borders indicate fields with photometry available for analysis presented in this paper.

identified stars in OGLE-III and OGLE-IV images indicates the internal accuracy of the astrometry at the  $0''.1$  level.

OGLE-IV observations cover the largest area overlapping with the sky surveyed by the GBS compared to the previous OGLE phases. However, because of some small “dead” regions on the sky caused by the gaps between detectors of the OGLE-IV mosaic camera and the lack of OGLE-IV photometric databases from a few fields closest to the Galactic plane which still await calibration, supplementary optical data from the OGLE-II (Udalski, Kubiak and Szymański 1997) and OGLE-III (Udalski 2003) phases were also analyzed. These two datasets were also collected with the 1.3-m Warsaw telescope at Las Campanas Observatory but with previous generation CCD cameras. OGLE-II observations were conducted in the

years 1997-2000 and OGLE-III 2001-2009 with typical cadence of one/two observations per night. It is worth noting that while the bright unsaturated limit of the OGLE-III and OGLE-IV photometry is approximately similar, OGLE-II data cover up to 1–1.5 mag brighter objects.

### 3. Search for the Optical Counterparts to the X-ray Sources

Search for optical counterparts to the GBS survey X-ray sources was performed in a few steps. First, based on the X-ray positions we selected a subsample of X-ray sources that fall into the regions of the sky for which OGLE-IV databases are currently available. From 1234 sources listed in the GBS catalog 836 passed this cut. However, a subset of this sample cannot be searched for variability. Some of the X-ray sources are located in the gaps between the CCD detectors of the OGLE-IV mosaic camera on the reference images, some are located so close to the edges of the observed area that due to imperfections of the telescope pointing the number of collected observations is too small for variability analysis. After removing such X-ray sources, we were left with a total of 782 objects for further analysis.

In the second step, we removed from the sample all cases where the X-ray position closely points to a bright object which is overexposed on the OGLE-IV reference image and thus its photometry is unavailable. In most cases the coincidence of the X-ray and optical positions is so good that these stars are very likely the optical counterparts to the X-ray sources. Photometry from shallow surveys like the ASAS survey (Pojmański 2002) should be checked to search for variability in this subsample. There were 87 such cases in our OGLE-IV sample and they were removed in this step.

Finally, we retrieved the OGLE-IV photometry of all objects located within the conservative radius of 15 pixels ( $3''.9$ ) around the X-ray position for all the remaining sources. The size of the circle is well over  $3\sigma$  X-ray position error for the vast majority of the analyzed X-ray sources. Depending on the stellar density of the field, from a few to several dozen objects were extracted inside each circle.

All extracted stars were searched for optical variability. First we performed a period search to extract periodic variables. We used the FNPEAKS code kindly provided by Z. Kołaczkowski and, independently, the code based on AOV algorithm (Schwarzenberg-Czerny 1989). After the determination of tentative periodicities all these objects were visually inspected and the periods were refined, if necessary. Next, all the non-periodic stars were also inspected visually to look for irregular variable stars. Finally, the positions of all selected variable stars were double checked on the reference images and subtracted images to verify correct identification of each variable object. It is well known that close neighbors blended with a variable star can mimic its variability.

205 variable sources were found within the  $3''.9$  radius of the positions of X-ray sources detected by the GBS project in the OGLE-IV dataset. These objects are very likely their optical counterparts.

Additionally, we repeated the same procedure for the OGLE-III and OGLE-II datasets. Positions of 114 and 58 GBS X-ray sources point to OGLE-III and OGLE-II fields, respectively. Eleven additional X-ray sources could be checked in the OGLE-III dataset including nine objects located outside currently available OGLE-IV fields and two objects in the OGLE-IV “dead” zones. No variable objects were found, however, in the searched areas. For 30 variable objects selected in the OGLE-IV data search OGLE-III photometry was retrieved extending the photometric coverage of these candidates to over a decade.

Six X-ray sources not covered by the OGLE-IV data as well as two sources from OGLE-IV “dead” zones were checked in the OGLE-II photometric databases. One new variable was cross-identified with a GBS X-ray source. For 18 variable objects found in the OGLE-IV data search OGLE-II light curves could also be retrieved.

Additionally, because the OGLE-II photometry has brighter saturation level all saturated in OGLE-IV potential counterparts were rechecked in the OGLE-II databases (nine objects). Three new variables were found among this bright stars sample increasing the total number of variable objects – OGLE optical counterpart candidates to GBS X-ray sources – to 209.

#### 4. Discussion

We performed tentative classification of each discovered variable star based on its photometric behavior. Initially, the variables were divided into two broad categories: those with periodic and irregular variability. From the former group a few sub-categories, sometimes overlapping, were then assigned.

The most numerous sub-group – 81 objects – consists of spotted stars with characteristic pattern of photometric behavior resembling RS CVn type stars. In most cases, we register only the variability caused by spots (rotation, almost synchronized with orbital period in the binary systems) and their slow migration on the stellar surface. However, the classical eclipsing RS CVn type stars are also present in our sample. Typical light curves of spotted stars are shown in Fig. 2.

The second group consists of pulsating red giants (OGLE Small Amplitude Red Giants, OSARGs, SemiRegular Variables, SRVs, Miras - *cf.* Soszyński *et al.* 2011b) – 25 objects. Such stars can be members of X-ray binary systems with a compact companion and accreting processes. Fig. 3 presents typical light curves of objects from this sub-category.

Eclipsing stars subgroup includes 36 objects with clear eclipses. Contact and detached short period binary systems are usually chromospherically active due to fast rotation tidally synchronized with the short orbital period and as a consequence – strong X-ray sources. Upper panels of Fig. 4 show the sample light curves of stars from this class.

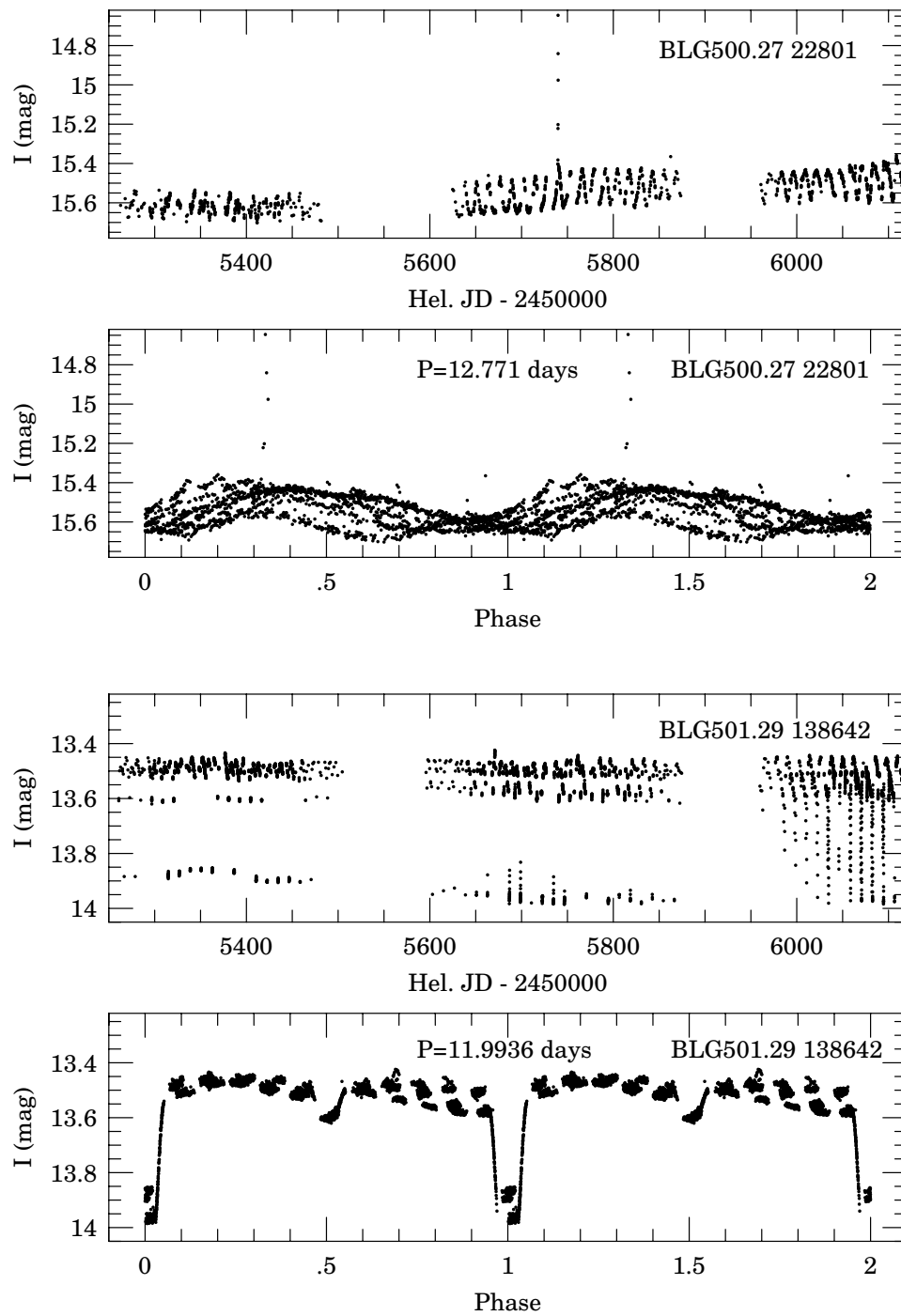


Fig. 2. Light curves of spotted stars. Two *upper panels* show time series and phased with the period 12.771 days light curve of the optical counterpart candidate (BLG500.27 22801) to the GBS #29 X-ray source. Two *bottom panels* show the light curves of the eclipsing system BLG501.29 138642 ( $P = 11.9936$  days) – a counterpart to the GBS #701 X-ray source.

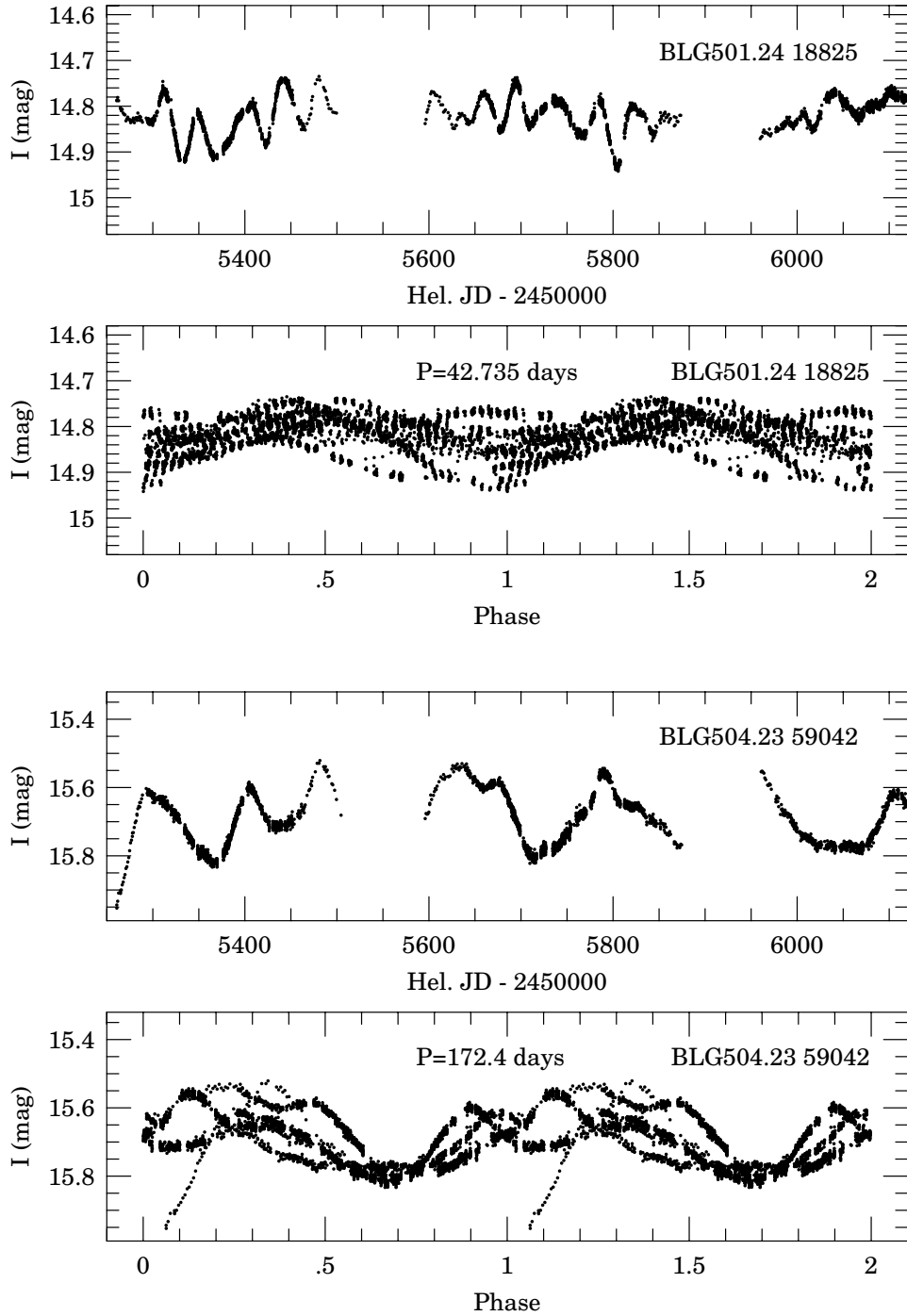


Fig. 3. Light curves of pulsating red giants. Two upper panels show time series and phased with the period 42.735 days light curve of the OSARG-type optical counterpart candidate (BLG501.24 18825) to the GBS #715 X-ray source. Two bottom panels show the light curves of the SRV candidate (BLG504.23 59042;  $P = 172.4$  days) to the GBS #907 X-ray source.



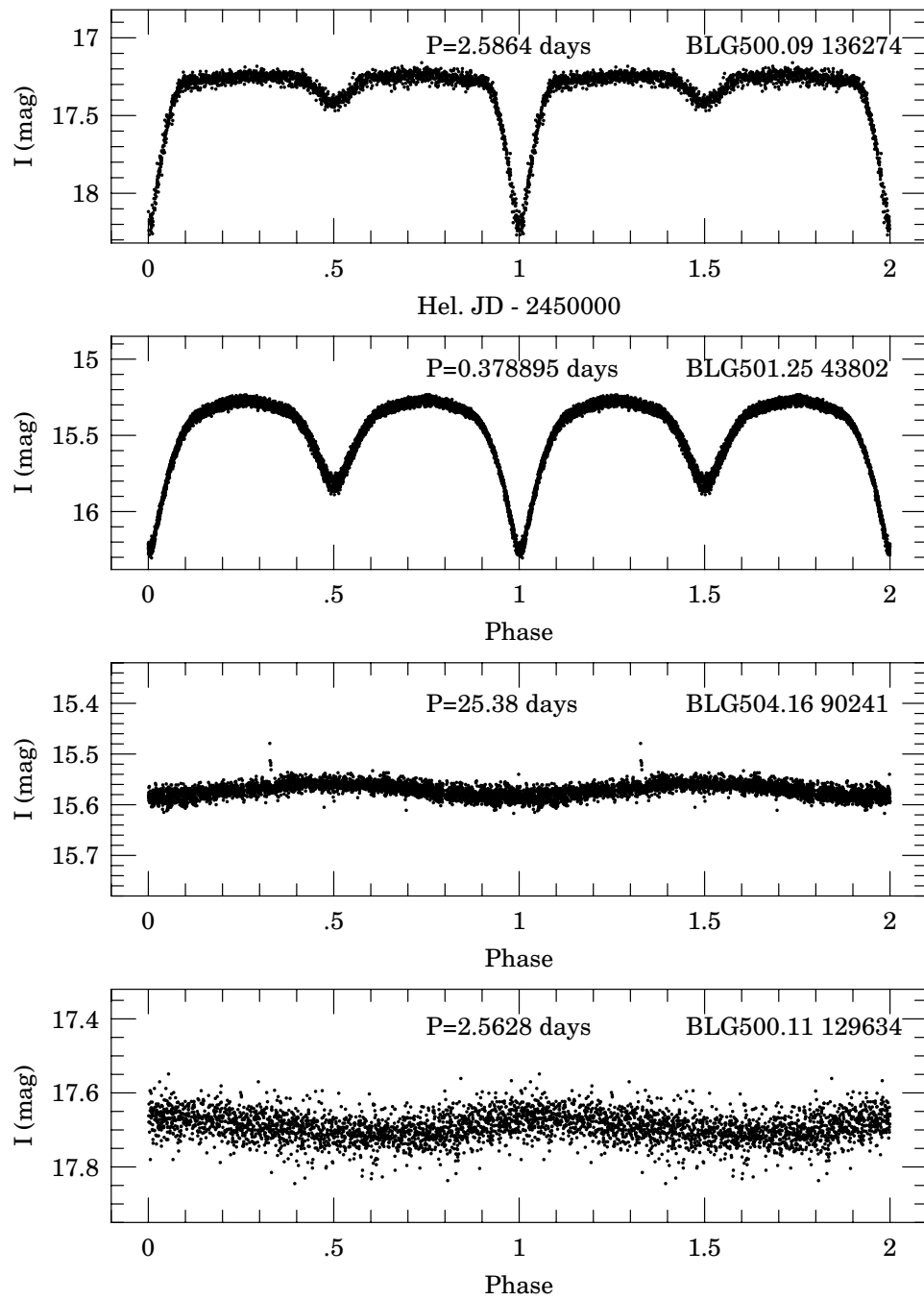


Fig. 4. Phased light curves of eclipsing and periodic counterpart candidates to the GBS X-ray sources: GBS #684 (BLG500.09 136274), GBS #152 (BLG501.25 43802), GBS #289 (BLG504.16 90241) and GBS #428 (BLG500.11 129634).

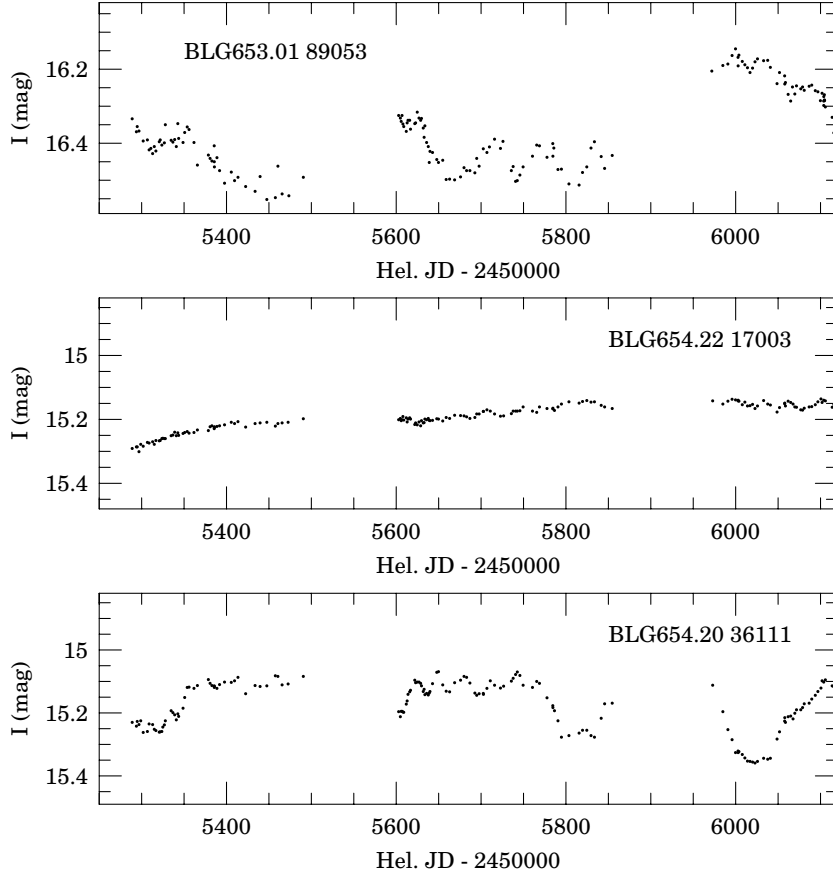


Fig. 5. Time series of the irregular counterpart candidates to the GBS X-ray sources: GBS #2 (BLG653.01 89053, Seyfert galaxy GRS 1734–292), GBS #212 (BLG654.22.17003) and GBS #332 (BLG654.20.36111).

Two RR Lyr pulsating stars, one of RRab and one of RRc type, were also found in the selected sample of variable stars. Although pulsating stars (Cepheids, RR Lyr) can potentially be soft X-ray emitters only a handful of Cepheids and RR Lyr stars have been detected in the X-ray band so far (Engle and Guinan 2012). Our detection of the coincidence of the positions of two RR Lyr stars with X-ray sources, could be thus an important discovery. However, we suspect that this may be a by chance coincidence. The number of RR Lyr stars detected in the typical Galactic bulge field analyzed in this paper is about 40 per  $2048 \times 4102$  pixel OGLE-IV CCD chip according to Soszyński *et al.* (2011a) OGLE Catalog of Variable Stars. Thus, we may expect about two RR Lyr variable star detections in the probed circle of 15 pixel radius in about 700 random directions toward the Galactic center. Close examination of the finding charts also suggest a by chance coincidence – both RR Lyr stars are relatively far from the X-ray position, one almost at the boundary of the searched circle.

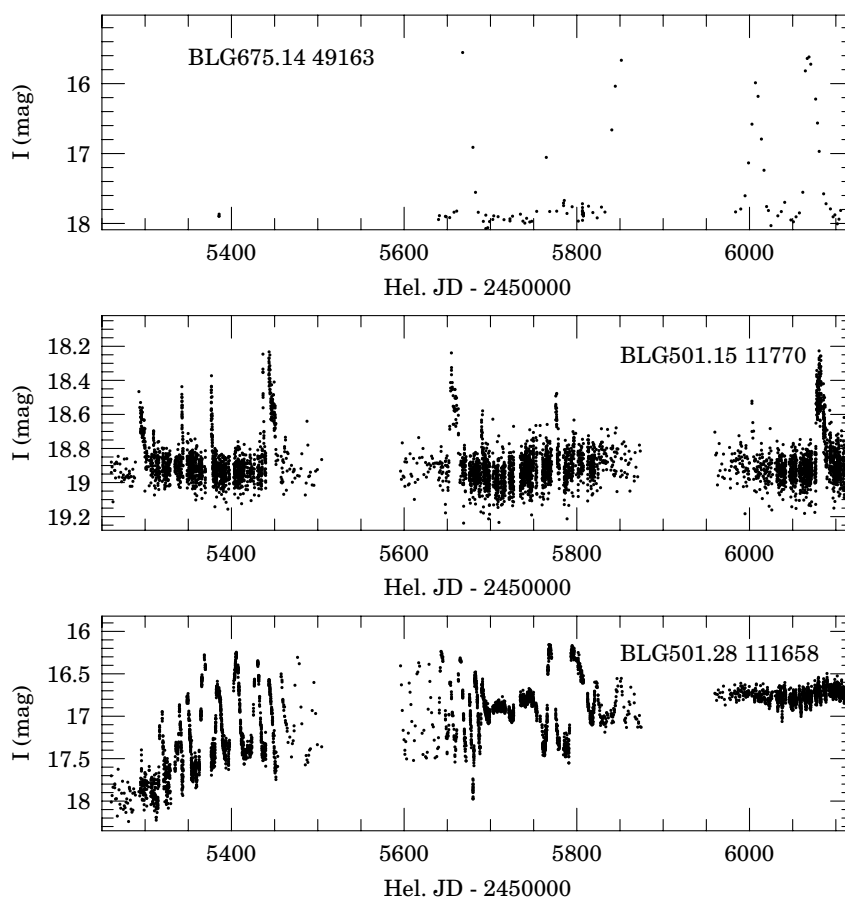


Fig. 6. Light curves of cataclysmic variables – optical counterpart candidates to the X-ray sources: GBS #18 (BLG675.14 49163), GBS #714 (BLG501.15 11770) and GBS #426 (BLG501.28 111658).

The variability of the remaining periodic stars (48 objects) may be caused either by the orbital motion (ellipsoidal variations), if they are binaries, or by the rotation. In the case of ellipsoidal variation the real period is twice of that found. Typical examples of stars from this group are shown in the bottom panels of Fig. 4.

Irregular variables form a separate group. This kind of variability may be an indicator of accreting systems like high or low mass X-ray binaries or nova-like variables (flickering). It cannot be ruled out, however, that some of the objects from this subgroup are actually quasi-periodic but the small number of observations collected so far prevented sound period detection.

It is also worth noticing that the optical counterpart to the GBS #2 source, which is a known Seyfert galaxy, GRS 1734–292 (Martí *et al.* 1998), is classified as irregular variable. OGLE provides, thus, long term optical monitoring of this interesting AGN. Three examples of irregular variables from this subgroup, including the counterpart of GBS #2, are shown in Fig. 5.

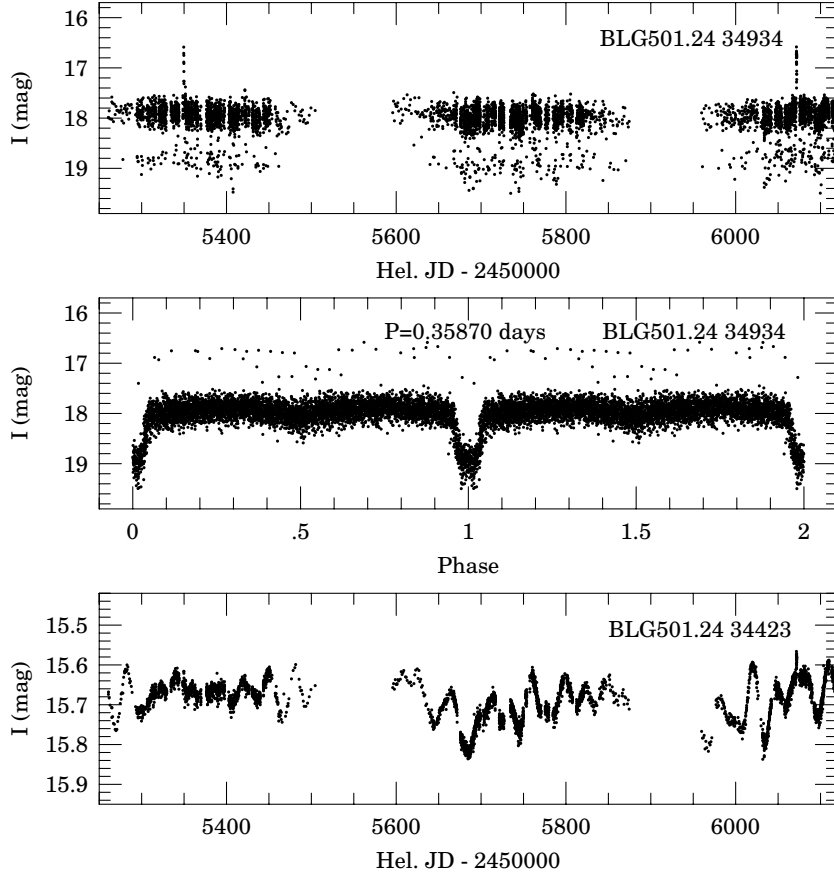


Fig. 7. Light curves of optical counterpart candidates to the X-ray source GBS #19. *Upper and middle panels*: eclipsing system BLG501.24 34934. *Lower panel*: pulsating red giant BLG501.24 34423.

We also found three classical cataclysmic variables, two typical dwarf novae and one Z Cam type star. Cataclysmic variables are well known X-ray emitters so the detection of these stars near the X-ray sources position clearly indicates that they are optical counterparts to these X-ray sources. Fig. 6 shows the light curves of these eruptive variables.

Table 1 lists all the X-ray sources from the GBS catalog cross-identified with OGLE variable objects. For each optical counterpart candidate the OGLE equatorial coordinates and distance from the X-ray source (in arcsecs) are provided, its mean optical photometry ( $I$ -band magnitude,  $V - I$  color, if available), period in days in the case of periodic variable stars and classification. Entries of counterpart candidates found in the OGLE-II databases are marked with italic font.

It should be noted that in the case of five X-ray sources from the GBS catalog more than one variable star were found within our search radius. The best example here is the X-ray source GBS #19 (Fig. 7). A variable red giant and

Table 1

Optical counterparts to the X-ray sources detected by the Galactic Bulge Survey revealing optical variability

GBS ID	OGLE-IV Field	OGLE-IV No	RA [2000.0]	DEC [2000.0]	$D$ ["]	$I$ [mag]	$V-I$ [mag]	$P$ [days]	Remarks
2	BLG653.01	89053	17 <sup>h</sup> 37 <sup>m</sup> 28 <sup>s</sup> .38	-29°08'02"1	0.16	16.422	-	-	I AGN
16	BLG504.24	65	17 <sup>h</sup> 55 <sup>m</sup> 45 <sup>s</sup> .84	-27°58'13"9	0.18	14.572	2.383	4.95	SP
18	BLG675.14	49163	17 <sup>h</sup> 39 <sup>m</sup> 35 <sup>s</sup> .76	-27°29'35"9	0.15	17.819	-	-	CV
19	BLG501.24	34423	17 <sup>h</sup> 49 <sup>m</sup> 54 <sup>s</sup> .52	-29°43'35"8	0.66	15.668	5.938	31.65	OSARG
19	BLG501.24	34934	17 <sup>h</sup> 49 <sup>m</sup> 54 <sup>s</sup> .63	-29°43'35"4	0.87	17.983	1.519	0.3587	E
23	BLG675.02	36509	17 <sup>h</sup> 42 <sup>m</sup> 31 <sup>s</sup> .57	-27°43'48"3	0.88	14.960	-	44.63	OSARG
24	BLG501.16	59134	17 <sup>h</sup> 48 <sup>m</sup> 49 <sup>s</sup> .50	-30°01'10"3	0.40	12.342	1.711	24.038	SP
29	BLG500.27	22801	17 <sup>h</sup> 53 <sup>m</sup> 41 <sup>s</sup> .90	-28°03'53"7	0.37	15.619	2.134	12.771	SP
56	BLG501.32	6608	17 <sup>h</sup> 50 <sup>m</sup> 00 <sup>s</sup> .36	-29°24'12"7	1.23	13.706	2.558	21.436	E SP
65	BLG500.13	14897	17 <sup>h</sup> 51 <sup>m</sup> 35 <sup>s</sup> .26	-28°43'45"3	0.42	12.977	0.909	0.70676	SP
71	BLG675.06	5524	17 <sup>h</sup> 39 <sup>m</sup> 49 <sup>s</sup> .29	-27°54'20"6	0.28	14.056	-	-	I
89	BLG653.11	44462	17 <sup>h</sup> 36 <sup>m</sup> 24 <sup>s</sup> .28	-28°45'32"7	0.24	14.228	-	18.382	SP
103	BLG501.29	50854	17 <sup>h</sup> 51 <sup>m</sup> 55 <sup>s</sup> .79	-29°23'10"1	3.72	14.714	1.684	-	I
106	BLG500.08	191736	17 <sup>h</sup> 54 <sup>m</sup> 34 <sup>s</sup> .47	-28°41'48"9	0.37	12.908	1.676	32.57329	SP
122	BLG653.08	10840	17 <sup>h</sup> 38 <sup>m</sup> 37 <sup>s</sup> .16	-28°45'44"9	0.44	13.369	-	43.668	SP
124	<i>BUL_SC5</i>	<i>134677</i>	<i>17<sup>h</sup>50<sup>m</sup>07<sup>s</sup>.00</i>	<i>-30°01'53"9</i>	<i>0.77</i>	<i>12.481</i>	<i>2.097</i>	-	<i>I</i>
127	BLG500.18	12184	17 <sup>h</sup> 54 <sup>m</sup> 21 <sup>s</sup> .19	-28°30'02"2	2.87	16.552	3.901	144.93	P
133	BLG501.29	45257	17 <sup>h</sup> 52 <sup>m</sup> 01 <sup>s</sup> .41	-29°25'07"9	1.04	13.191	3.700	19.292	OSARG
134	BLG648.28	31469	17 <sup>h</sup> 47 <sup>m</sup> 14 <sup>s</sup> .97	-26°16'49"0	0.05	13.711	-	18.526	OSARG
137	BLG504.14	157126	17 <sup>h</sup> 55 <sup>m</sup> 53 <sup>s</sup> .26	-28°16'33"9	0.69	15.113	1.315	0.43104	E SP
143	BLG675.26	84886	17 <sup>h</sup> 42 <sup>m</sup> 49 <sup>s</sup> .73	-26°48'23"0	0.23	13.946	-	1.72473	P
144	BLG654.25	20335	17 <sup>h</sup> 33 <sup>m</sup> 00 <sup>s</sup> .32	-29°36'14"9	0.47	14.469	-	2.47771	E
152	BLG501.25	43802	17 <sup>h</sup> 48 <sup>m</sup> 56 <sup>s</sup> .72	-29°38'35"9	1.05	15.461	1.384	0.378895	E
155	BLG504.07	23237	17 <sup>h</sup> 55 <sup>m</sup> 42 <sup>s</sup> .07	-28°27'39"5	0.69	16.515	2.057	0.53454	E
163	BLG504.15	66246	17 <sup>h</sup> 55 <sup>m</sup> 32 <sup>s</sup> .43	-28°04'31"4	0.33	15.041	2.501	2.02896	E
174	BLG654.27	54219	17 <sup>h</sup> 36 <sup>m</sup> 58 <sup>s</sup> .35	-29°23'51"7	1.33	12.848	-	217.4	P
180	BLG500.20	154077	17 <sup>h</sup> 52 <sup>m</sup> 20 <sup>s</sup> .78	-28°23'40"6	0.56	13.544	-	2.5896	E
185	BLG654.21	59612	17 <sup>h</sup> 35 <sup>m</sup> 27 <sup>s</sup> .56	-29°45'16"6	0.53	12.936	-	44.25	P
190	BLG653.12	5	17 <sup>h</sup> 35 <sup>m</sup> 44 <sup>s</sup> .39	-28°54'00"4	0.92	14.678	-	225.2	MIRA
195	BLG654.30	14819	17 <sup>h</sup> 35 <sup>m</sup> 07 <sup>s</sup> .54	-29°19'05"1	0.29	14.712	-	28.5	E
196	BLG500.07	1605	17 <sup>h</sup> 50 <sup>m</sup> 03 <sup>s</sup> .35	-29°11'50"4	1.28	17.089	1.854	1.9972	SP
200	BLG504.16	58311	17 <sup>h</sup> 54 <sup>m</sup> 45 <sup>s</sup> .46	-28°07'43"6	2.79	18.350	-	72.464	P
203	BLG653.05	39870	17 <sup>h</sup> 34 <sup>m</sup> 55 <sup>s</sup> .60	-28°58'56"9	2.11	13.949	-	9.38086	SP
204	BLG500.10	172048	17 <sup>h</sup> 53 <sup>m</sup> 12 <sup>s</sup> .45	-28°47'46"5	0.97	15.267	1.692	2.014	SP
212	BLG654.22	17003	17 <sup>h</sup> 35 <sup>m</sup> 10 <sup>s</sup> .15	-29°36'06"1	0.78	15.209	-	-	I
216	BLG653.09	79513	17 <sup>h</sup> 37 <sup>m</sup> 21 <sup>s</sup> .71	-28°53'57"3	0.32	13.216	-	16.42036	SP
222	BLG648.16	1012	17 <sup>h</sup> 44 <sup>m</sup> 05 <sup>s</sup> .45	-27°00'13"3	0.11	15.514	-	46.083	SP
227	BLG501.28	155033	17 <sup>h</sup> 52 <sup>m</sup> 19 <sup>s</sup> .58	-29°21'09"8	0.08	14.191	2.300	2.947	SP
228	BLG534.32	97586	17 <sup>h</sup> 49 <sup>m</sup> 24 <sup>s</sup> .63	-30°34'44"7	0.42	13.089	1.835	29.916	SP
231	BLG648.28	36747	17 <sup>h</sup> 47 <sup>m</sup> 14 <sup>s</sup> .73	-26°09'38"2	0.25	13.140	-	69.32	OSARG
234	BLG675.28	21714	17 <sup>h</sup> 41 <sup>m</sup> 47 <sup>s</sup> .68	-26°46'49"8	2.86	16.539	-	26.455	P
237	BLG654.17	56669	17 <sup>h</sup> 38 <sup>m</sup> 15 <sup>s</sup> .98	-29°39'39"9	0.72	14.138	-	0.273483	E
240	BLG654.21	7912	17 <sup>h</sup> 35 <sup>m</sup> 47 <sup>s</sup> .78	-29°43'33"2	0.56	12.523	-	-	I
253	BLG504.25	87539	17 <sup>h</sup> 54 <sup>m</sup> 27 <sup>s</sup> .60	-27°47'32"9	0.89	12.689	0.943	1.31734	E SP
282	BLG653.11	550	17 <sup>h</sup> 36 <sup>m</sup> 34 <sup>s</sup> .43	-28°53'33"9	0.05	18.322	-	9.72760	P
289	BLG504.16	90151	17 <sup>h</sup> 54 <sup>m</sup> 39 <sup>s</sup> .15	-28°08'50"0	0.32	14.723	2.400	11.84	SP
289	BLG504.16	90241	17 <sup>h</sup> 54 <sup>m</sup> 38 <sup>s</sup> .88	-28°08'51"4	3.56	15.575	4.250	25.38	P
295	BLG500.10	186047	17 <sup>h</sup> 53 <sup>m</sup> 11 <sup>s</sup> .01	-28°42'27"7	0.25	13.432	1.689	2.92227	SP

Table 1

Continued

GBS ID	OGLE-IV Field	OGLE-IV No	RA [2000.0]	DEC [2000.0]	$D$ ["]	$I$ [mag]	$V-I$ [mag]	$P$ [days]	Remarks
300	BLG654.14	66787	17 <sup>h</sup> 33 <sup>m</sup> 51 <sup>s</sup> .57	-30°06'30".9	0.62	15.282	-	21.1417	SP
303	BLG504.31	31226	17 <sup>h</sup> 56 <sup>m</sup> 02 <sup>s</sup> .11	-27°39'21".2	2.17	12.753	1.213	0.8313	SP
304	BLG504.31	31226	17 <sup>h</sup> 56 <sup>m</sup> 02 <sup>s</sup> .11	-27°39'21".2	1.57	12.753	1.213	0.8313	SP
326	BLG675.20	61377	17 <sup>h</sup> 41 <sup>m</sup> 31 <sup>s</sup> .36	-27°09'59".2	0.32	13.827	-	0.23462	P
330	BLG653.19	81200	17 <sup>h</sup> 36 <sup>m</sup> 43 <sup>s</sup> .88	-28°21'21".3	0.82	15.069	-	-	I
331	BLG654.28	28452	17 <sup>h</sup> 36 <sup>m</sup> 23 <sup>s</sup> .47	-29°22'34".7	0.14	17.277	-	18.215	SP
332	BLG654.20	36111	17 <sup>h</sup> 36 <sup>m</sup> 20 <sup>s</sup> .20	-29°33'38".9	0.80	15.156	-	-	I
336	BLG654.04	45052	17 <sup>h</sup> 35 <sup>m</sup> 31 <sup>s</sup> .42	-30°24'23".3	0.38	15.696	-	9.99	SP
354	BLG500.18	172616	17 <sup>h</sup> 53 <sup>m</sup> 52 <sup>s</sup> .75	-28°25'13".2	0.79	15.092	2.074	8.21018	SP
362	<i>BUL_SC5</i>	284655	17 <sup>h</sup> 50 <sup>m</sup> 37 <sup>s</sup> .53	-29°40'45".5	0.26	11.420	2.272	107.53	P
363	BLG501.31	34121	17 <sup>h</sup> 50 <sup>m</sup> 33 <sup>s</sup> .73	-29°21'33".5	0.35	14.005	1.679	8.7413	SP
375	BLG675.17	11128	17 <sup>h</sup> 43 <sup>m</sup> 57 <sup>s</sup> .95	-27°10'34".0	1.00	15.365	-	62.8	SP
387	BLG654.27	27852	17 <sup>h</sup> 37 <sup>m</sup> 05 <sup>s</sup> .58	-29°24'52".5	0.86	13.044	-	4.831	P
391	BLG654.11	47010	17 <sup>h</sup> 36 <sup>m</sup> 06 <sup>s</sup> .42	-30°03'11".0	0.33	13.977	-	11.47	E SP
395	BLG654.31	30300	17 <sup>h</sup> 34 <sup>m</sup> 18 <sup>s</sup> .96	-29°28'33".8	1.12	14.868	-	5.965	SP
397	BLG654.23	61348	17 <sup>h</sup> 33 <sup>m</sup> 59 <sup>s</sup> .54	-29°49'47".2	0.50	13.190	-	0.77471	E
414	BLG504.30	6878	17 <sup>h</sup> 57 <sup>m</sup> 09 <sup>s</sup> .75	-27°32'49".7	0.25	13.715	1.585	0.40826	SP
416	BLG504.16	83867	17 <sup>h</sup> 54 <sup>m</sup> 35 <sup>s</sup> .04	-28°11'52".5	1.43	14.998	-	16.5563	P
417	BLG504.16	130997	17 <sup>h</sup> 54 <sup>m</sup> 27 <sup>s</sup> .75	-28°07'49".3	0.29	13.749	0.532	0.95923	P
426	BLG501.28	111658	17 <sup>h</sup> 52 <sup>m</sup> 36 <sup>s</sup> .05	-29°19'39".9	0.17	17.293	0.439	-	CV
428	BLG500.11	129634	17 <sup>h</sup> 52 <sup>m</sup> 32 <sup>s</sup> .88	-28°37'48".5	0.55	17.698	1.710	2.56279	P
429	BLG500.20	120943	17 <sup>h</sup> 52 <sup>m</sup> 32 <sup>s</sup> .43	-28°21'01".1	0.28	16.839	2.037	10.94092	SP
432	BLG500.13	29005	17 <sup>h</sup> 51 <sup>m</sup> 19 <sup>s</sup> .17	-28°53'08".9	0.49	14.163	1.781	11.876	SP
434	BLG500.05	84278	17 <sup>h</sup> 51 <sup>m</sup> 10 <sup>s</sup> .63	-29°01'17".7	0.62	14.479	1.101	0.69871	SP
439	BLG534.25	65908	17 <sup>h</sup> 48 <sup>m</sup> 40 <sup>s</sup> .65	-30°55'53".2	1.75	16.443	-	64.516	SRV
472	BLG675.22	60741	17 <sup>h</sup> 40 <sup>m</sup> 25 <sup>s</sup> .65	-27°05'40".4	0.29	14.623	-	21.834	SP
483	BLG654.26	59596	17 <sup>h</sup> 37 <sup>m</sup> 31 <sup>s</sup> .10	-29°24'28".8	3.47	13.476	-	0.6462	E
484	BLG654.19	17980	17 <sup>h</sup> 37 <sup>m</sup> 19 <sup>s</sup> .57	-29°33'23".8	0.57	16.433	-	7.062	SP
491	BLG653.04	15499	17 <sup>h</sup> 35 <sup>m</sup> 43 <sup>s</sup> .46	-29°03'11".8	1.99	14.561	-	16.10306	P
494	BLG654.05	47692	17 <sup>h</sup> 34 <sup>m</sup> 58 <sup>s</sup> .69	-30°13'29".0	1.74	16.667	-	-	I
495	BLG654.22	76376	17 <sup>h</sup> 34 <sup>m</sup> 47 <sup>s</sup> .61	-29°35'10".5	2.09	16.623	-	0.48629	P
497	BLG654.14	1240	17 <sup>h</sup> 34 <sup>m</sup> 22 <sup>s</sup> .10	-30°05'05".9	0.20	14.057	-	3.4965	SP
500	BLG654.16	68256	17 <sup>h</sup> 32 <sup>m</sup> 39 <sup>s</sup> .40	-30°02'22".7	0.22	15.163	-	1.8954	P
501	BLG500.11	55525	17 <sup>h</sup> 52 <sup>m</sup> 52 <sup>s</sup> .63	-28°48'05".4	0.67	14.142	1.975	15.03759	SP
502	BLG500.20	154130	17 <sup>h</sup> 52 <sup>m</sup> 23 <sup>s</sup> .57	-28°24'10".9	1.38	15.218	1.471	6.9252	SP
505	BLG648.16	31001	17 <sup>h</sup> 43 <sup>m</sup> 53 <sup>s</sup> .28	-26°53'53".7	0.67	13.048	-	11.147	SP
513	BLG504.22	107805	17 <sup>h</sup> 56 <sup>m</sup> 46 <sup>s</sup> .04	-27°45'47".6	0.25	13.097	2.450	11.8343	OSARG
515	BLG504.24	65	17 <sup>h</sup> 55 <sup>m</sup> 45 <sup>s</sup> .84	-27°58'13".9	3.14	14.572	2.383	4.95	SP
516	BLG504.24	57283	17 <sup>h</sup> 55 <sup>m</sup> 34 <sup>s</sup> .69	-27°47'59".7	3.12	15.751	-	33.333	SRV
522	BLG500.17	158208	17 <sup>h</sup> 54 <sup>m</sup> 32 <sup>s</sup> .61	-28°29'19".6	1.96	12.971	5.007	147.3	SRV
526	BLG500.01	144233	17 <sup>h</sup> 54 <sup>m</sup> 01 <sup>s</sup> .04	-29°00'46".2	3.71	15.429	2.513	135.1	P
532	BLG500.21	2338	17 <sup>h</sup> 52 <sup>m</sup> 15 <sup>s</sup> .84	-28°34'15".3	0.73	12.890	1.873	44.25	SP
538	BLG501.22	116664	17 <sup>h</sup> 50 <sup>m</sup> 54 <sup>s</sup> .10	-29°46'16".0	0.60	13.799	1.176	6.0533	SP
543	BLG501.24	78370	17 <sup>h</sup> 49 <sup>m</sup> 32 <sup>s</sup> .70	-29°49'55".9	0.41	14.280	2.918	61.35	SP
556	BLG648.29	41317	17 <sup>h</sup> 46 <sup>m</sup> 30 <sup>s</sup> .18	-26°22'04".4	0.20	14.675	-	-	I
561	BLG648.30	8035	17 <sup>h</sup> 46 <sup>m</sup> 07 <sup>s</sup> .68	-26°15'47".1	0.54	16.121	-	12.4915	E
575	BLG648.14	72850	17 <sup>h</sup> 44 <sup>m</sup> 59 <sup>s</sup> .28	-26°51'10".2	0.68	14.951	-	6.5147	SP
594	BLG675.18	76442	17 <sup>h</sup> 42 <sup>m</sup> 46 <sup>s</sup> .29	-27°13'53".3	0.16	16.472	-	27.322	SP
611	BLG675.23	21477	17 <sup>h</sup> 39 <sup>m</sup> 50 <sup>s</sup> .50	-27°09'16".5	1.70	13.201	-	1.3776	P
611	BLG675.23	21504	17 <sup>h</sup> 39 <sup>m</sup> 50 <sup>s</sup> .34	-27°09'17".3	2.98	14.793	-	-	I
633	BLG654.15	41782	17 <sup>h</sup> 33 <sup>m</sup> 18 <sup>s</sup> .72	-30°05'22".3	0.67	14.615	-	0.73185	P
634	BLG654.24	67281	17 <sup>h</sup> 33 <sup>m</sup> 16 <sup>s</sup> .65	-29°40'03".2	0.20	14.744	-	0.76104	SP

Table 1

Continued

GBS ID	OGLE-IV Field	OGLE-IV No	RA [2000.0]	DEC [2000.0]	$D$ ["]	$I$ [mag]	$V-I$ [mag]	$P$ [days]	Remarks
637	BLG654.15	75839	17 <sup>h</sup> 33 <sup>m</sup> 08 <sup>s</sup> .55	-29°57'27".6	1.21	13.429	-	4.97018	P
642	BLG504.14	192340	17 <sup>h</sup> 55 <sup>m</sup> 55 <sup>s</sup> .14	-28°01'58".9	1.12	14.924	1.948	2.924	SP
649	BLG504.15	98233	17 <sup>h</sup> 55 <sup>m</sup> 24 <sup>s</sup> .65	-28°10'36".8	0.79	13.431	2.935	30.67485	SP
650	BLG500.09	64937	17 <sup>h</sup> 54 <sup>m</sup> 08 <sup>s</sup> .51	-28°48'28".8	3.29	12.849	4.751	31.5	SRV
651	BLG648.28	48495	17 <sup>h</sup> 47 <sup>m</sup> 03 <sup>s</sup> .70	-26°11'08".8	0.18	13.485	-	-	I
657	BLG504.29	15566	17 <sup>h</sup> 57 <sup>m</sup> 46 <sup>s</sup> .88	-27°33'09".8	0.39	16.280	1.562	16.58375	P
659	BLG645.04	31747	17 <sup>h</sup> 57 <sup>m</sup> 38 <sup>s</sup> .37	-27°19'55".2	0.28	14.556	-	74.627	SP
663	BLG504.30	69448	17 <sup>h</sup> 56 <sup>m</sup> 30 <sup>s</sup> .96	-27°31'39".9	0.53	13.495	2.450	24.691	SP
666	BLG504.23	118900	17 <sup>h</sup> 56 <sup>m</sup> 01 <sup>s</sup> .69	-27°44'48".8	0.49	14.104	1.522	2.6201	E SP
668	BLG504.14	188107	17 <sup>h</sup> 55 <sup>m</sup> 55 <sup>s</sup> .86	-28°05'55".5	0.41	14.147	2.669	106.4	SP
674	BLG504.24	74705	17 <sup>h</sup> 55 <sup>m</sup> 19 <sup>s</sup> .78	-27°56'32".5	1.07	14.868	-	24.73	OSARG
676	BLG500.17	159235	17 <sup>h</sup> 54 <sup>m</sup> 32 <sup>s</sup> .45	-28°28'13".4	3.73	17.241	2.748	0.30728	RRLYR
679	BLG500.18	50697	17 <sup>h</sup> 54 <sup>m</sup> 13 <sup>s</sup> .98	-28°33'41".6	3.68	15.111	3.425	-	I
681	BLG500.09	128064	17 <sup>h</sup> 54 <sup>m</sup> 05 <sup>s</sup> .63	-28°47'32".6	0.04	13.865	0.826	2.0736	SP
684	BLG500.09	136274	17 <sup>h</sup> 54 <sup>m</sup> 00 <sup>s</sup> .38	-28°43'32".4	2.47	17.369	2.566	2.5864	E SP
685	BLG500.09	128146	17 <sup>h</sup> 53 <sup>m</sup> 56 <sup>s</sup> .51	-28°46'58".3	0.58	14.760	1.345	2.7894	SP
688	BLG500.19	348	17 <sup>h</sup> 53 <sup>m</sup> 42 <sup>s</sup> .30	-28°35'31".8	0.63	16.640	3.175	8.231	SP
689	BLG500.19	17579	17 <sup>h</sup> 53 <sup>m</sup> 39 <sup>s</sup> .84	-28°29'31".6	0.36	13.825	1.525	189	P
691	BLG500.19	125229	17 <sup>h</sup> 53 <sup>m</sup> 24 <sup>s</sup> .21	-28°27'10".8	1.20	19.629	-	2.794	P
692	BLG500.02	163813	17 <sup>h</sup> 53 <sup>m</sup> 05 <sup>s</sup> .18	-29°13'00".6	1.33	14.609	3.796	93.3	P
695	BLG501.28	64217	17 <sup>h</sup> 52 <sup>m</sup> 40 <sup>s</sup> .19	-29°20'57".8	0.26	15.703	2.757	0.30988	P
701	BLG501.29	138642	17 <sup>h</sup> 51 <sup>m</sup> 41 <sup>s</sup> .10	-29°18'55".2	0.77	13.531	1.838	11.9936	E SP
702	BLG500.12	122438	17 <sup>h</sup> 51 <sup>m</sup> 39 <sup>s</sup> .41	-28°52'43".5	0.44	15.540	1.560	1.50011	E
<b>705</b>	BLG501.30	35398	17 <sup>h</sup> 51 <sup>m</sup> 16 <sup>s</sup> .15	-29°23'44".4	0.87	15.975	1.579	-	I
<b>705</b>	BLG501.30	35400	17 <sup>h</sup> 51 <sup>m</sup> 15 <sup>s</sup> .91	-29°23'42".8	2.76	15.400	-	326.8	MIRA
711	BLG501.31	34198	17 <sup>h</sup> 50 <sup>m</sup> 32 <sup>s</sup> .49	-29°21'00".1	0.68	15.649	2.322	13.73	SP
712	BLG501.14	108924	17 <sup>h</sup> 50 <sup>m</sup> 14 <sup>s</sup> .77	-30°03'19".5	0.76	15.556	2.485	6.84	SP
714	BLG501.15	11770	17 <sup>h</sup> 49 <sup>m</sup> 59 <sup>s</sup> .31	-29°57'11".1	0.71	18.874	-	-	CV
715	BLG501.24	18825	17 <sup>h</sup> 49 <sup>m</sup> 59 <sup>s</sup> .15	-29°34'38".1	0.79	14.836	-	42.735	OSARG
717	BLG501.24	35909	17 <sup>h</sup> 49 <sup>m</sup> 50 <sup>s</sup> .32	-29°42'30".4	2.92	18.600	-	0.54767	RRLYR*
718	BLG501.07	45474	17 <sup>h</sup> 49 <sup>m</sup> 48 <sup>s</sup> .54	-30°12'21".0	0.65	15.335	1.437	5.824	P
721	BLG534.32	107583	17 <sup>h</sup> 49 <sup>m</sup> 20 <sup>s</sup> .74	-30°28'05".9	0.34	15.633	-	2.66207	E
724	<i>BUL_SC44</i>	<i>12986</i>	<i>17<sup>h</sup>48<sup>m</sup>54<sup>s</sup>.26</i>	<i>-30°18'39".5</i>	<i>0.51</i>	<i>12.827</i>	<i>1.104</i>	<i>0.32200</i>	<i>E</i>
742	BLG648.29	69672	17 <sup>h</sup> 46 <sup>m</sup> 19 <sup>s</sup> .94	-26°12'28".7	0.11	14.430	-	0.25321	P
774	BLG675.17	4519	17 <sup>h</sup> 44 <sup>m</sup> 01 <sup>s</sup> .34	-27°16'46".8	3.57	14.530	-	43.47826	P
778	BLG648.16	78697	17 <sup>h</sup> 43 <sup>m</sup> 35 <sup>s</sup> .43	-26°48'57".1	0.44	17.822	-	6.079	P
794	BLG675.03	22881	17 <sup>h</sup> 41 <sup>m</sup> 42 <sup>s</sup> .38	-27°58'30".3	0.78	19.209	-	0.11786	E?
796	BLG675.03	73380	17 <sup>h</sup> 41 <sup>m</sup> 27 <sup>s</sup> .62	-27°58'39".2	0.48	14.229	-	1.06571	E
800	BLG675.04	85070	17 <sup>h</sup> 40 <sup>m</sup> 51 <sup>s</sup> .59	-27°45'59".7	0.32	13.954	-	213	MIRA
809	BLG675.22	60737	17 <sup>h</sup> 40 <sup>m</sup> 17 <sup>s</sup> .79	-27°06'07".8	1.26	14.581	-	35.7	P
811	BLG675.14	28661	17 <sup>h</sup> 39 <sup>m</sup> 48 <sup>s</sup> .50	-27°24'16".0	0.59	14.668	-	43.3	P
819	BLG675.07	56138	17 <sup>h</sup> 38 <sup>m</sup> 56 <sup>s</sup> .46	-27°48'33".4	0.36	16.978	-	35	SP
829	BLG654.26	41915	17 <sup>h</sup> 37 <sup>m</sup> 38 <sup>s</sup> .06	-29°21'44".8	0.42	15.767	-	-	I
830	BLG653.26	52494	17 <sup>h</sup> 37 <sup>m</sup> 29 <sup>s</sup> .94	-28°07'59".5	0.58	13.127	-	8.288	E
837	BLG653.19	61176	17 <sup>h</sup> 36 <sup>m</sup> 47 <sup>s</sup> .64	-28°22'21".7	2.41	15.714	-	15.18	P
843	BLG654.03	59545	17 <sup>h</sup> 36 <sup>m</sup> 05 <sup>s</sup> .70	-30°18'16".8	3.27	14.403	-	49.5	OSARG
845	BLG654.29	2771	17 <sup>h</sup> 35 <sup>m</sup> 47 <sup>s</sup> .48	-29°29'15".0	0.08	16.443	-	3.158	P
847	BLG654.12	30313	17 <sup>h</sup> 35 <sup>m</sup> 37 <sup>s</sup> .78	-29°56'01".3	1.00	14.470	-	17.212	P
848	BLG654.04	55881	17 <sup>h</sup> 35 <sup>m</sup> 33 <sup>s</sup> .43	-30°17'44".0	0.42	18.294	-	7.4405	SP
852	BLG654.13	32681	17 <sup>h</sup> 35 <sup>m</sup> 02 <sup>s</sup> .21	-30°03'54".7	0.93	14.742	-	0.29857	P
853	BLG654.13	74975	17 <sup>h</sup> 34 <sup>m</sup> 46 <sup>s</sup> .94	-29°56'31".6	0.64	16.118	-	0.91405	E

\* OGLE-BLG-RRLYR-03686 (Soszyński *et al.* 2011a)

Table 1

Concluded

GBS ID	OGLE-IV Field	OGLE-IV No	RA [2000.0]	DEC [2000.0]	$D$ ["]	$I$ [mag]	$V-I$ [mag]	$P$ [days]	Remarks
858	BLG654.24	63566	17 <sup>h</sup> 33 <sup>m</sup> 26 <sup>s</sup> .90	-29°42'11".7	0.27	15.403	-	11.174	SP
869	BLG648.13	45934	17 <sup>h</sup> 45 <sup>m</sup> 36 <sup>s</sup> .79	-26°51'32".7	0.31	14.130	-	23.81	SP
877	BLG504.24	106420	17 <sup>h</sup> 55 <sup>m</sup> 14 <sup>s</sup> .65	-27°59'01".4	0.36	12.763	2.472	27.933	SP
878	BLG501.24	8191	17 <sup>h</sup> 50 <sup>m</sup> 01 <sup>s</sup> .72	-29°42'56".7	0.71	15.848	1.646	0.64616	E
895	BLG654.23	73640	17 <sup>h</sup> 34 <sup>m</sup> 05 <sup>s</sup> .41	-29°42'43".8	0.81	15.979	-	0.42973	E
896	BLG645.03	63999	17 <sup>h</sup> 58 <sup>m</sup> 12 <sup>s</sup> .28	-27°21'39".3	0.77	13.707	-	3.8534	E
898	BLG504.29	96872	17 <sup>h</sup> 57 <sup>m</sup> 28 <sup>s</sup> .81	-27°33'10".7	0.60	14.798	3.099	44.84	SP
899	BLG504.29	118157	17 <sup>h</sup> 57 <sup>m</sup> 18 <sup>s</sup> .94	-27°36'08".7	0.34	12.976	3.020	49.751	SP
901	BLG504.30	59047	17 <sup>h</sup> 56 <sup>m</sup> 51 <sup>s</sup> .19	-27°23'50".6	0.75	13.094	0.829	0.39967	E
906	BLG504.31	26678	17 <sup>h</sup> 56 <sup>m</sup> 16 <sup>s</sup> .81	-27°26'34".2	0.55	13.798	2.126	0.29347	SP
907	BLG504.23	59042	17 <sup>h</sup> 56 <sup>m</sup> 11 <sup>s</sup> .47	-27°52'33".5	3.43	15.710	-	172.4	SRV
908	BLG504.31	22399	17 <sup>h</sup> 56 <sup>m</sup> 10 <sup>s</sup> .29	-27°32'58".1	1.08	17.148	-	67.1	SRV
909	BLG504.31	20360	17 <sup>h</sup> 56 <sup>m</sup> 09 <sup>s</sup> .94	-27°35'17".5	0.42	15.969	2.516	4.0967	SP
910	BLG504.23	90667	17 <sup>h</sup> 56 <sup>m</sup> 07 <sup>s</sup> .52	-27°57'26".4	0.23	15.288	1.947	1.24425	SP
912	BLG504.31	42181	17 <sup>h</sup> 56 <sup>m</sup> 03 <sup>s</sup> .86	-27°28'33".6	0.62	15.458	2.346	0.37699	P
914	BLG504.31	33921	17 <sup>h</sup> 55 <sup>m</sup> 59 <sup>s</sup> .55	-27°37'44".9	0.65	13.769	0.833	-	I
915	BLG504.31	58984	17 <sup>h</sup> 55 <sup>m</sup> 58 <sup>s</sup> .61	-27°29'56".8	2.29	16.630	1.647	1.1609	P
924	BLG500.17	36873	17 <sup>h</sup> 55 <sup>m</sup> 00 <sup>s</sup> .48	-28°19'56".5	0.20	13.777	1.991	77.5	P
926	BLG504.16	57832	17 <sup>h</sup> 54 <sup>m</sup> 49 <sup>s</sup> .47	-28°07'36".6	0.42	17.195	2.210	3.787	P
929	BLG500.17	144211	17 <sup>h</sup> 54 <sup>m</sup> 30 <sup>s</sup> .83	-28°33'35".5	0.19	16.227	1.695	0.59379	SP
930	BLG500.17	151398	17 <sup>h</sup> 54 <sup>m</sup> 29 <sup>s</sup> .31	-28°31'52".8	2.99	16.716	1.665	-	I
933	BLG500.09	120810	17 <sup>h</sup> 54 <sup>m</sup> 05 <sup>s</sup> .77	-28°48'23".4	2.27	15.607	3.306	-	I
938	BLG500.09	190630	17 <sup>h</sup> 53 <sup>m</sup> 52 <sup>s</sup> .05	-28°44'52".7	1.33	13.735	0.786	2.42096	E
940	BLG500.19	52204	17 <sup>h</sup> 53 <sup>m</sup> 30 <sup>s</sup> .09	-28°32'47".7	0.39	15.330	1.337	-	I
944	BLG500.28	13	17 <sup>h</sup> 52 <sup>m</sup> 54 <sup>s</sup> .34	-28°16'29".9	2.48	14.334	5.269	42.02	SRV
946	BLG500.11	55525	17 <sup>h</sup> 52 <sup>m</sup> 52 <sup>s</sup> .63	-28°48'05".4	3.22	14.142	1.975	15.03759	SP
947	BLG500.03	89767	17 <sup>h</sup> 52 <sup>m</sup> 45 <sup>s</sup> .16	-28°59'15".1	3.42	15.918	5.493	14.881	OSARG
948	BLG500.03	100501	17 <sup>h</sup> 52 <sup>m</sup> 41 <sup>s</sup> .86	-29°12'52".6	0.36	14.925	1.430	1.9577	SP
953	BLG500.21	34612	17 <sup>h</sup> 52 <sup>m</sup> 03 <sup>s</sup> .78	-28°33'51".1	0.34	15.901	1.534	1.0989	SP
955	BLG500.12	106387	17 <sup>h</sup> 51 <sup>m</sup> 51 <sup>s</sup> .42	-28°42'46".5	0.35	16.386	-	-	I
964	<i>BUL_SC5</i>	<i>172053</i>	<i>17<sup>h</sup>50<sup>m</sup>15<sup>s</sup>.31</i>	<i>-29°39'13".8</i>	<i>0.19</i>	<i>12.289</i>	<i>1.681</i>	<i>81.97</i>	<i>P</i>
966	BLG501.15	49578	17 <sup>h</sup> 49 <sup>m</sup> 42 <sup>s</sup> .67	-30°02'44".5	1.96	16.881	3.170	9.662	SP
969	BLG501.15	71683	17 <sup>h</sup> 49 <sup>m</sup> 32 <sup>s</sup> .21	-30°03'50".4	0.60	18.335	-	32.154	P
970	BLG501.24	80876	17 <sup>h</sup> 49 <sup>m</sup> 28 <sup>s</sup> .07	-29°46'29".1	0.70	12.504	0.970	-	I
972	BLG534.32	100700	17 <sup>h</sup> 49 <sup>m</sup> 23 <sup>s</sup> .67	-30°32'16".2	0.30	12.755	0.921	0.334094	E
973	BLG501.16	69	17 <sup>h</sup> 49 <sup>m</sup> 21 <sup>s</sup> .61	-30°07'39".2	0.45	16.672	2.838	10.352	SP
978	BLG501.25	42282	17 <sup>h</sup> 48 <sup>m</sup> 59 <sup>s</sup> .54	-29°39'40".0	2.32	16.675	1.708	1.05765	P
981	BLG501.16	49689	17 <sup>h</sup> 48 <sup>m</sup> 54 <sup>s</sup> .94	-29°54'16".7	0.51	15.823	1.335	91.7	P
1019	BLG648.13	46396	17 <sup>h</sup> 45 <sup>m</sup> 48 <sup>s</sup> .53	-26°50'50".5	0.18	16.406	-	0.35143	E
1033	BLG648.31	60638	17 <sup>h</sup> 45 <sup>m</sup> 02 <sup>s</sup> .19	-26°14'49".4	0.23	13.104	-	54.07799	SP
1070	BLG675.26	56707	17 <sup>h</sup> 42 <sup>m</sup> 58 <sup>s</sup> .73	-26°55'01".4	0.39	14.560	-	47.17	SP
1071	BLG675.01	49220	17 <sup>h</sup> 42 <sup>m</sup> 57 <sup>s</sup> .12	-27°46'30".2	0.55	15.767	-	37.175	P
1074	BLG675.26	74928	17 <sup>h</sup> 42 <sup>m</sup> 52 <sup>s</sup> .61	-26°57'14".1	0.96	15.156	-	3.1616	E
1078	BLG675.19	37341	17 <sup>h</sup> 42 <sup>m</sup> 24 <sup>s</sup> .03	-27°11'57".8	2.61	16.536	-	-	I
1086	BLG675.03	34167	17 <sup>h</sup> 41 <sup>m</sup> 46 <sup>s</sup> .47	-27°49'54".7	0.03	16.526	-	11.768	E
1090	BLG675.11	107190	17 <sup>h</sup> 41 <sup>m</sup> 25 <sup>s</sup> .07	-27°31'43".6	0.67	14.827	-	49.26	SP
1104	BLG675.21	104241	17 <sup>h</sup> 40 <sup>m</sup> 40 <sup>s</sup> .67	-27°08'07".9	3.88	15.119	-	109.89	P
1110	BLG675.13	40278	17 <sup>h</sup> 40 <sup>m</sup> 17 <sup>s</sup> .69	-27°30'57".1	0.44	13.617	-	30.612	E
1112	BLG675.22	79334	17 <sup>h</sup> 40 <sup>m</sup> 12 <sup>s</sup> .92	-27°12'35".7	1.26	14.275	-	17.699	SP
1151	BLG653.01	1611	17 <sup>h</sup> 37 <sup>m</sup> 55 <sup>s</sup> .27	-29°10'10".1	2.67	14.616	-	78.125	SRV
<b>1155</b>	BLG654.26	59596	17 <sup>h</sup> 37 <sup>m</sup> 31 <sup>s</sup> .10	-29°24'28".8	0.38	13.476	-	0.6462	E
<b>1155</b>	BLG654.26	59618	17 <sup>h</sup> 37 <sup>m</sup> 31 <sup>s</sup> .33	-29°24'28".9	3.35	15.531	-	56.8	SRV



Table 1  
Concluded

GBS ID	OGLE-IV Field	OGLE-IV No	RA [2000.0]	DEC [2000.0]	<i>D</i> ["]	<i>I</i> [mag]	<i>V</i> − <i>I</i> [mag]	<i>P</i> [days]	Remarks
1161	BLG653.19	67406	17 <sup>h</sup> 36 <sup>m</sup> 45 <sup>s</sup> .56	−28°34′14″.8	3.15	15.511	−	94.3	SRV
1165	BLG653.20	10600	17 <sup>h</sup> 36 <sup>m</sup> 33 <sup>s</sup> .67	−28°30′03″.9	0.14	13.703	−	74.1	SRV
1168	BLG654.03	26666	17 <sup>h</sup> 36 <sup>m</sup> 27 <sup>s</sup> .84	−30°12′14″.1	0.52	13.823	−	65.79	P
1179	BLG654.11	52361	17 <sup>h</sup> 36 <sup>m</sup> 06 <sup>s</sup> .21	−29°55′40″.5	2.14	15.369	−	−	I
1185	BLG653.12	9604	17 <sup>h</sup> 35 <sup>m</sup> 48 <sup>s</sup> .65	−28°47′09″.7	0.94	14.880	−	2.1497	E
1187	BLG653.04	7005	17 <sup>h</sup> 35 <sup>m</sup> 45 <sup>s</sup> .73	−29°08′02″.7	2.71	15.012	−	16.92	OSARG
1194	BLG654.04	62415	17 <sup>h</sup> 35 <sup>m</sup> 27 <sup>s</sup> .50	−30°14′01″.3	2.51	16.015	−	1.91022	SP
1208	BLG654.06	16127	17 <sup>h</sup> 34 <sup>m</sup> 23 <sup>s</sup> .71	−30°17′05″.1	0.90	14.935	−	24.876	SP
1228	BLG500.03	188094	17 <sup>h</sup> 52 <sup>m</sup> 31 <sup>s</sup> .10	−28°58′03″.9	1.58	14.929	2.458	3.4235	P
1229	BLG500.12	106361	17 <sup>h</sup> 51 <sup>m</sup> 56 <sup>s</sup> .83	−28°41′45″.7	0.34	14.649	1.770	−	I

- Italic font entry highlights the counterpart candidates selected from the OGLE-II databases.
- Boldface GBS number highlights the cases when two variable stars are located in the search region.
- Variability type abbreviations: SP – spotted star, OSARG/SRV/MIRA – pulsating giant, E – eclipsing system, P – periodic system, RRLYR – RR Lyr pulsating star, CV – cataclysmic variable, I – irregular star, AGN – active galactic nucleus.
- The same optical counterpart candidates for two close GBS X-ray sources: GBS #16/GBS #515, GBS #303/GBS #304, GBS #483/GBS #1155, GBS #501/GBS #946.

fainter eclipsing system are detected very close to the X-ray position. Only further, preferably spectroscopic, observations may solve the cross-identification ambiguity in this case. However, it may turn out that both these stars are X-ray sources. A one day long flare of  $\approx 1$  mag amplitude observed on  $\text{HJD} = 2455349.7$  and  $\text{HJD} = 2456071.7$  in the eclipsing star may indicate stellar activity. On the other hand the light curve of the red giant resembles that of other X-ray binary systems.

There are also four cases where two separate X-rays sources from the GBS catalog point very close to each other (*e.g.*, #16 and #515 are separated by only  $3.''3$ ). In such cases the same optical variable stars are selected as potential counterparts to these X-ray sources. Additional observations can resolve the issue of the real connections of the sources in such cases.

Fig. 8 shows the histogram of the angular distances between the OGLE equatorial coordinates of the counterpart candidates and their X-ray positions in  $0.''1$  bins. It is clearly seen that for the vast majority of objects the coincidence of positions is better than  $1.''$ . In the remaining cases it is possible that the X-ray coordinates are less accurate or a variable optical candidate is aligned by chance on the sky with the corresponding X-ray source. Conservative selection of the 15 pixel ( $3.''9$ ) radius ensures high completeness of our search.

Finally, it is worth noticing that in the case of 19 X-ray sources where we did not find any optically variable objects in their neighborhood, the position of the X-ray source points with a high accuracy – better than  $0.''75$  – to a well separated

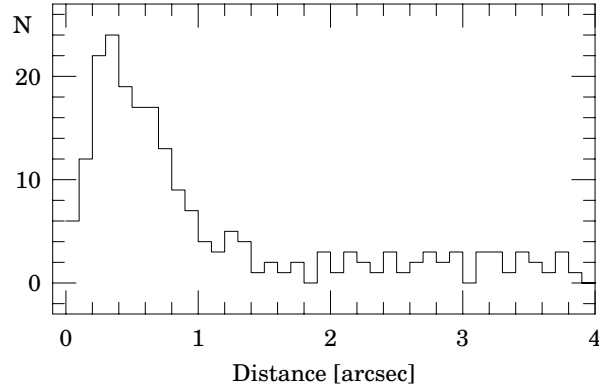


Fig. 8. Histogram of the angular distances in the sky between the OGLE and X-ray position of the optical counterpart candidates. The bin size is  $0.''1$ .

Table 2

Possible bright non-variable optical counterparts to the X-ray sources detected by the Galactic Bulge Survey

GBS ID	OGLE-IV Field	OGLE-IV No	RA [2000.0]	DEC [2000.0]	$D$ ["]	$I$ [mag]	$V-I$ [mag]
88	BLG654.24	96086	17 <sup>h</sup> 33 <sup>m</sup> 08 <sup>s</sup> .04	-29°37'52".7	0.36	15.423	-
149	BLG675.27	31995	17 <sup>h</sup> 42 <sup>m</sup> 26 <sup>s</sup> .78	-26°47'31".3	0.57	12.636	-
170	BLG654.18	34390	17 <sup>h</sup> 37 <sup>m</sup> 55 <sup>s</sup> .18	-29°35'40".3	0.13	12.980	-
294	BLG504.25	67635	17 <sup>h</sup> 54 <sup>m</sup> 35 <sup>s</sup> .37	-27°44'59".4	0.49	14.041	1.783
393	BLG654.29	66612	17 <sup>h</sup> 35 <sup>m</sup> 30 <sup>s</sup> .83	-29°18'31".9	0.23	14.145	-
403	BLG500.02	184262	17 <sup>h</sup> 53 <sup>m</sup> 06 <sup>s</sup> .53	-29°05'30".1	0.33	14.384	1.055
454	BLG648.23	8019	17 <sup>h</sup> 45 <sup>m</sup> 25 <sup>s</sup> .15	-26°39'08".0	0.49	12.490	-
631	BLG653.05	53272	17 <sup>h</sup> 34 <sup>m</sup> 43 <sup>s</sup> .92	-29°09'49".7	0.60	13.521	-
646	BLG654.30	12088	17 <sup>h</sup> 35 <sup>m</sup> 06 <sup>s</sup> .17	-29°21'12".1	0.36	13.802	-
662	BLG504.22	107804	17 <sup>h</sup> 56 <sup>m</sup> 42 <sup>s</sup> .18	-27°45'54".3	0.10	13.144	1.859
675	BLG500.17	150996	17 <sup>h</sup> 54 <sup>m</sup> 34 <sup>s</sup> .00	-28°32'19".7	0.36	13.360	0.906
773	BLG648.16	12494	17 <sup>h</sup> 44 <sup>m</sup> 01 <sup>s</sup> .99	-26°50'49".7	0.75	13.285	-
880	BLG501.16	47309	17 <sup>h</sup> 49 <sup>m</sup> 00 <sup>s</sup> .89	-29°54'32".8	0.22	13.102	0.794
967	BLG534.32	76738	17 <sup>h</sup> 49 <sup>m</sup> 37 <sup>s</sup> .15	-30°32'57".8	0.34	13.074	0.719
1045	BLG648.32	45146	17 <sup>h</sup> 44 <sup>m</sup> 29 <sup>s</sup> .95	-26°19'49".5	0.29	15.861	-
1049	BLG648.16	1014	17 <sup>h</sup> 44 <sup>m</sup> 08 <sup>s</sup> .94	-26°59'58".6	0.35	15.554	-
1123	BLG675.06	51526	17 <sup>h</sup> 39 <sup>m</sup> 38 <sup>s</sup> .91	-27°43'56".5	0.15	16.286	-
1200	BLG654.22	10352	17 <sup>h</sup> 35 <sup>m</sup> 13 <sup>s</sup> .17	-29°40'23".8	0.27	14.655	-
1209	BLG654.31	13876	17 <sup>h</sup> 34 <sup>m</sup> 23 <sup>s</sup> .62	-29°21'55".0	0.67	13.471	-

star brighter than 16.5 mag. Therefore, it is very likely that these stars may also be potential optical counterparts. As can be seen from the light curves in the OGLE X-ray optical counterparts monitoring system, XROM (Udalski 2008), many optical counterparts to the X-ray sources can be optically quiet for years. Table 2 lists these potential non-variable optical counterparts to the X-ray sources.

Table 1 can be a good starting point for further follow-up observations of the selected optical counterparts. In particular extracting new low-mass and massive X-ray binaries would be of great importance for further studies of these objects in the Galactic center environment. We plan to include a subsample of the most interesting objects presented here to the list of objects monitored regularly by the OGLE XROM system (Udalski 2008). This can facilitate follow-up observations providing information on the current optical behavior of the observed objects.

## 5. Data Availability

The OGLE-IV photometric data presented in this paper are available to the astronomical community from the OGLE Internet Archive:

*http://ogle.astrouw.edu.pl*  
*ftp://ftp.astrouw.edu.pl/ogle4/XRAY-GBS/*

Usage of the data is allowed under the proper acknowledgment to the OGLE project.

**Acknowledgements.** The OGLE project has received funding from the European Research Council under the European Community's Seventh Framework Programme (FP7/2007-2013)/ERC grant agreement No. 246678 to AU.

## REFERENCES

- Alard, C., and Lupton, R. 1998, *ApJ*, **503**, 325.  
 Alard, C. 2000, *A&AS*, **144**, 363.  
 Coe, M.J., Edge, W.R.T., Galache, J.L., and McBride, V.A. 2005, *MNRAS*, **356**, 502.  
 Engle, S.G., and Guinan, E.F. 2012, *Journal of Astronomy and Space Sciences*, **29**, 181.  
 Jonker, P.G., *et al.* 2011, *ApJS*, **194**, 18.  
 Kozłowski, S., *et al.* 2012, *ApJ*, **746**, 27.  
 Martí, J., Mirabel, I.F., Chaty, S., and Rodriguez, L.F. 1998, *A&A*, **330**, 72.  
 Pojmański, G. 2002, *Acta Astron.*, **52**, 397.  
 Schwarzenberg-Czerny, A. 1989, *MNRAS*, **241**, 153.  
 Soszyński, I., *et al.* 2011a, *Acta Astron.*, **61**, 1.  
 Soszyński, I., *et al.* 2011b, *Acta Astron.*, **61**, 217.  
 Szymański, M.K., Udalski, A., Soszyński, I., Kubiak, M., Pietrzyński, G., Poleski, R., Wyrzykowski, Ł., and Ulaczyk, K. 2011, *Acta Astron.*, **61**, 83.  
 Udalski, A., Kubiak, M., and Szymański, M. 1997, *Acta Astron.*, **47**, 319.  
 Udalski, A. 2003, *Acta Astron.*, **53**, 291.  
 Udalski, A. 2008, *Acta Astron.*, **58**, 187.  
 Watson, M.G., *et al.* 2009, *A&A*, **493**, 339.  
 Wozniak, P.R. 2000, *Acta Astron.*, **50**, 421.